Pentameric structure and subunit stoichiometry of a neuronal nicotinic acetylcholine receptor

Cooper, Ellis; Couturier-Goebel, Sabine; Ballivet, Marc

How to cite

COOPER, Ellis, COUTURIER-GOEBEL, Sabine, BALLIVET, Marc. Pentameric structure and subunit stoichiometry of a neuronal nicotinic acetylcholine receptor. In: Nature, 1991, vol. 350, n° 6315, p. 235–238. doi: 10.1038/350235a0

This publication URL: https://archive-ouverte.unige.ch/unige:104942
Publication DOI: 10.1038/350235a0

of a mixture other than 1:9 (below), we will see that it is highly unlikely that any of the hybrid channels are weakly sensitive like the pure mutant channel.

We can now predict the subunit stoichiometry, n, of the Shaker K^+ channel. Combining equations (3) and (4) and taking logarithms yields:

$$\frac{1}{\ln(f_{mut})}\ln\left(\frac{U_{mix}}{U_{mut}}\right) = n - \frac{1}{\ln(f_{mut})}\ln\left(1-\frac{R}{U_{mix}}\right) \quad (5)$$

Each quantity on the left-hand side of equation (5) is either known or is directly measurable. The value of the expression differs from n by a term whose magnitude depends on the value of R: as R approaches zero it will approach zero. Therefore, the expression will underestimate n, but will converge to n as U_{mix} and U_{mut} are determined at successively higher toxin concentrations. Figure 3*b* shows a plot of the values obtained upon substitution of U_{mix} (for $f_{mut}=0.9$) and U_{mut} into the expression on the left-hand side of equation (5). At high toxin concentrations the data points converge to a value near 4, consistent with a tetrameric channel structure. The curves in Fig. 3 are the best fits generated from the theory ($n=4$ provides a significantly better fit than does $n=3$ or 5). Most importantly, however, the asymptotic value is independent of *a priori* assumptions about the value of n or specific values of K_i.

Equation (5) can be tested by asking whether the same value for n is obtained using a different ratio of wild-type to mutant subunits. Table 1 shows that a value close to four is also obtained with a 2:8 mixture ($f_{mut}=0.8$). A very different value for U_{mix} is observed, but the difference is exactly compensated by the $1/\ln(f_{mut})$ term.

The results of this study provide evidence that the Shaker K^+ channel is a tetramer, on the basis of two assumptions. The first is that the wild-type and mutant subunits aggregate randomly. The similar properties and levels of expression of wild-type and mutant channels argue that this is plausible. The second assumption is that only the fully mutant form is weakly toxin sensitive in a mixing experiment. This is supported by the finding that the weakly sensitive fraction has the same toxin affinity as the pure D431N channel. However, if the hybrid channel containing only a single wild-type subunit (and $n-1$ mutant subunits) is weakly toxin sensitive like the fully mutant form, the data corresponding to $f_{mut}=0.9$ are consistent with a 12-subunit channel. However, the data corresponding to $f_{mut}=0.8$ are consistent with a 9-subunit channel. These two sets of data are simultaneously satisfied if the channel is a tetramer and all hybrid channels are toxin sensitive compared to the fully mutant form.

These results indicate that a single wild-type subunit confers upon the Shaker K^+ channel relatively high toxin sensitivity. This is initially surprising, but is explicable. The toxin is an asymmetric molecule[14] that binds to a receptor with fourfold symmetry. The toxin must therefore combine with the channel in four indistinguishable ways. If a bound toxin molecule interacts strongly with only one of the subunits at position 431, then a mutation on a single subunit simply reduces by one the number of ways that the toxin molecule can combine with the channel. Therefore, even with three mutant and only one wild-type subunits, the toxin may be expected to block the channel with one quarter of the affinity ($K_i=16$ nM). In fact, the inhibition constant for the channel containing a single wild-type subunit, estimated from the inhibition curve in Fig. 3*a*, is 19 nM.

It is interesting to compare the subunit stoichiometry of the Shaker K^+ channel (tetramer) with that of the nicotinic acetylcholine receptor ion channel (pentamer) and gap junction hemichannel (hexamer). The gap junction channel forms a very wide, nonselective pore that is about 16 Å in diameter[15,16]. The nicotinic acetylcholine receptor ion channel is selective for cations over anions and has an intermediate pore diameter of about 6.5–7 Å[17]. The voltage-gated K^+ channels, however, are highly selective and have a narrow ion conduction pore[17]. As was suggested by Unwin, there seems to be a simple relationship between the number of subunits in an ion channel and its pore diameter[18]. This correlation may be coincidental, but it is consistent with a crude model of an ion channel as a barrel with its subunits acting as the staves.

Note added in proof: It has recently been demonstrated that CTX prepared by a separate method inhibits the Shaker K^+ channel with low affinity[23]. The high-affinity inhibitor used in this study may therefore be a CTX isoform (there are many). This does not influence the conclusions reached here about the channel structure. □

Received 2 October 1990; accepted 22 January 1991.

1. Christie, M. J., North, R. A., Osborne, P. B., Douglass, J. & Adelman, J. P. *Neuron* **2**, 405–411 (1990).
2. Isacoff, E. Y., Jan, Y. N. & Jan, L. Y. *Nature* **345**, 530–534 (1990).
3. Ruppersberg, J. P. *et al. Nature* **345**, 535–537 (1990).
4. Tempel, B. L., Papazian, D. M., Schwarz, T. L., Jan, Y. N. & Jan, L. Y. *Science* **237**, 770–775 (1987).
5. Catterall, W. A. *Science* **242**, 50–61 (1988).
6. Agnew, W. S., *Nature* **331**, 114–115 (1988).
7. Miller, C., Moczydlowski, E., Latorre, R. & Phillips, M. *Nature* **313**, 316–318 (1985).
8. Anderson, C. S., MacKinnon, R., Smith, C. & Miller, C. *J. gen. Physiol.* **91**, 317–334 (1988).
9. MacKinnon, R. & Miller, C. *J. gen. Physiol.* **91**, 335–349 (1988).
10. Galvez, A. *et al. J. biol. Chem.* **265**, 11083–11090.
11. MacKinnon, R., Reinhart, P. & White, M. *Neuron* **1**, 997–1001 (1988).
12. MacKinnon, R. & Miller, C. *Science* **245**, 1382–1385 (1989).
13. MacKinnon, R., Heginbotham, L. & Abramson, T. *Neuron* **5**, 767–771 (1990).
14. Massefski, W., Redfield, A. G., Hare, D. R. & Miller, C. *Science* **249**, 449–596 (1990).
15. Neyton, J. & Trautmann, A. *Nature* **317**, 331–335 (1985).
16. Makowski, L., Caspar, D. L. D., Phillips, W. C. & Goodenough, D. A. *J. molec. Biol.* **174**, 449–481 (1984).
17. Hille, B. in *Ionic Channels in Excitable Membranes* 426 (Sinauer, Sunderland, Massachusetts, 1984).
18. Unwin, N. *Neuron* **3**, 665–676 (1989).
19. Kamb, A., Tseng-Crank, J. & Tanouye, M. A. *Neuron* **1**, 421–430 (1988).
20. Kunkel, T. A. *Proc. natn. Acad. Sci. U.S.A.* **82**, 488–492 (1985).
21. Sanger, F., Nicklen, S. & Coulson, A. R. *Proc. natn. Acad. Sci. U.S.A.* **74**, 5463–5467 (1977).
22. Bezanilla, F. & Armstrong, C. M. *J. gen. Physiol.* **70**, 549–566 (1977).
23. Oliva, C., Folander, K. & Smith, J. S. *Biophys. J.* **59**, 450a (1991).

ACKNOWLEDGEMENTS. I thank C. Miller, G. Yellen, and L. Heginbotham for their comments on the manuscript. This research was supported by the NIH.

Pentameric structure and subunit stoichiometry of a neuronal nicotinic acetylcholine receptor

Ellis Cooper, Sabine Couturier* & Marc Ballivet*

Department of Physiology, McGill University, Montréal, Québec H3G 1YG, Canada
* Department of Biochemistry, University of Geneva, 1211 Geneva 4, Switzerland

NEURONAL nicotinic acetylcholine receptors are members of a gene family of ligand-gated transmitter receptors that includes muscle nicotinic receptors, $GABA_A$ receptors and glycine receptors[1–4]. Several lines of evidence indicate that neuronal nicotinic receptors can be made up of only two subunits, an alpha (α) subunit which binds ligand, and a non-alpha (nα) or beta (β) subunit[5–13]. The stoichiometry of each subunit in the functional receptor has been difficult to assess, however. Estimates of the molecular weight of neuronal nicotonic receptor macromolecules suggest that these receptors contain at least four subunits but probably not more than five[5,12]. We have examined the subunit stoichiometry of the chick neuronal $\alpha_4/n\alpha_1$ receptor[7,9] by first using site-directed mutagenesis to create subunits that confer different single channel properties on the receptor. Co-injection with wild-type and mutant subunits led to the appearance of receptors with wild-type, mutant and hybrid conductances. From the number of hybrid conductances, we could deduce the number of each subunit in the functional receptor.

The M2 region of muscle nicotinic acetylcholine receptor (nAChR) subunits participates in the channel pore[14–18], and charged residues on either side of M2 influence the rate of ion transport through the channel[18]. We investigated whether

FIG. 1 The amino-acid sequence of the M2 domain for α_4 and $n\alpha_1$ subunits. The triplets encoding the residues in the boxes were mutated using standard procedures[21,22]; the numbers above the residues correspond to their position. The glutamic acid at 266 in the α_4 subunit was changed to a lysine and the mutated subunit is referred to as α_4K266. The lysine at 260 of the $n\alpha_1$ subunit was changed to a glutamic acid; this mutated subunit is referred to as $n\alpha_1$E260.

charged residues at the equivalent position on the α_4 and $n\alpha_1$ subunits have a similar effect on the conductance of the neuronal nAChR. Figure 1 shows the amino-acid sequence of the M2 region for the α_4 and $n\alpha_1$ subunits. The α_4 subunit has a negatively charged glutamic acid (E) at position 266, and the $n\alpha_1$ subunit has a positively charged lysine (K) at the equivalent position (260). Figure 2*a* shows the single channel conductance for the $\alpha_4/n\alpha_1$ receptor. These receptors form a single population with a conductance of 20 pS. Lower conductance states, like those reported for the rat α_2/β_2 and α_3/β_2 (ref. 19), were not observed.

To determine the effect of these charged residues on the rate of ion transport, we changed the lysine at position 260 of $n\alpha_1$ to a glutamic acid; we refer to this mutated subunit as $n\alpha_1$E260. Figure 2*b* shows that the $\alpha_4/n\alpha_1$E260 receptor has a single channel conductance of 37.5 pS, almost twice that of wild-type $\alpha_4/n\alpha_1$ receptors. In a parallel experiment, we changed the glutamic acid at position 266 of α_4 to a lysine; we refer to this mutated subunit as α_4K266. Figure 2*c* shows that the α_4K266/$n\alpha_1$E260 receptor has a single channel conductance of 17.5 pS, less than half that of the $\alpha_4/n\alpha_1$E260 receptor. These results establish that charged residues outside the M2 domain influence the rate of ion transport through the channel pore of neuronal nAChRs in a manner similar to muscle nAChRs; this also suggests that the structure of neuronal and muscle nAChRs may be similar. Direct comparisons of the magnitude of the charge change on the single channel conductance for neuronal nAChRs compared with muscle nAChRs are difficult because these experiments on $\alpha_4/n\alpha_1$ receptors could not be done in the absence of divalent cations.

To assess the number of α_4 subunits in the functional receptor, we co-injected complementary DNAs for α_4 and α_4K266 together with $n\alpha_1$E260 into oocytes. The rationale for this experiment is that in these oocytes some receptors will form that only

FIG. 2 Effect of mutations on the single channel conductance. This figure shows three receptors: *a*, $\alpha_4/n\alpha_1$ receptor; *b*, $\alpha_4/n\alpha_1$E260 receptor; *c*, α_4K266/$n\alpha_1$E260 receptor. For each receptor, the upper left shows single channels measured in outside-out patches at −120 mV holding potential; below is the amplitude histogram of over 200 openings measured at −120 mV. On the right is the *I–V* curve. Each point represents the mean of at least 36 openings, the s.e.m. are smaller than the symbols. The *I–V* curve for each receptor was constructed with data from 5–6 different patches which were held at 4–6 different holding potentials. The single channel conductances are: 20.2 pS for the $\alpha_4/n\alpha_1$ receptor in *a*; 37.5 pS for the $\alpha_4/n\alpha_1$E260 receptor in *b*; 17.5 pS for the α_4K266/$n\alpha_1$E260 receptor in *c*. The trace length of the single channel records in *a*, *b* and *c* is 100 ms.

METHODS. Nuclei of *Xenopus laevis* oocytes were co-injected with cDNAs for two subunits (in equal molar ratios)[23]: α_4 and $n\alpha_1$ in *a*, α_4 and $n\alpha_1$E260 in *b*; α_4K266 and $n\alpha_1$E260 in *c*. Single channel recordings were from outside-out patches at 22–24 °C with a List EPC-7 amplifier 2–5 days after injection[23]. Currents were digitized and stored on tape and analysed with a DEC PDP 11/73 computer. Currents were filtered at 1.5 kHz and sampled at 10 kHz. Amplitude histograms were constructed by measuring the amplitude of individual openings. A computer routine that fits single channels with idealized square pulses was used to measure the single channel amplitudes. Only openings longer than 1 ms and in which a plateau had been reached were included. Low doses of ACh were used to ensure that the probability of opening was small in order to reduce simultaneous openings. The amplitude histograms in Figs 3 and 4 were modelled as the sum of gaussian distributions and a nonlinear curve-fitting routine was used to judge the best fit for the parameters[24]. The means and variances of the largest and smallest distributions were constrained to the values obtained in the control experiments shown in Fig. 2, whereas the nonlinear fitting routine minimized the χ^2 to obtain estimations of the remaining parameters. In all outside-out patches, ACh currents ran down in 3–5 min after forming the patch. The bath solution was a modified Barth's medium (OR-2)[23], divalent-free, plus: 1 mM Ca^{2+}; 1 μM atropine; 10 mM HEPES (pH adjusted to 7.3–7.4 with NaOH); and 50–100 nM ACh. The patch pipette contained: 80 mM KF; 20 mM KAc; 10 mM EGTA; 10 mM HEPES (pH adjusted to 7.4 with NaOH, final Na concentration was 2 mM).

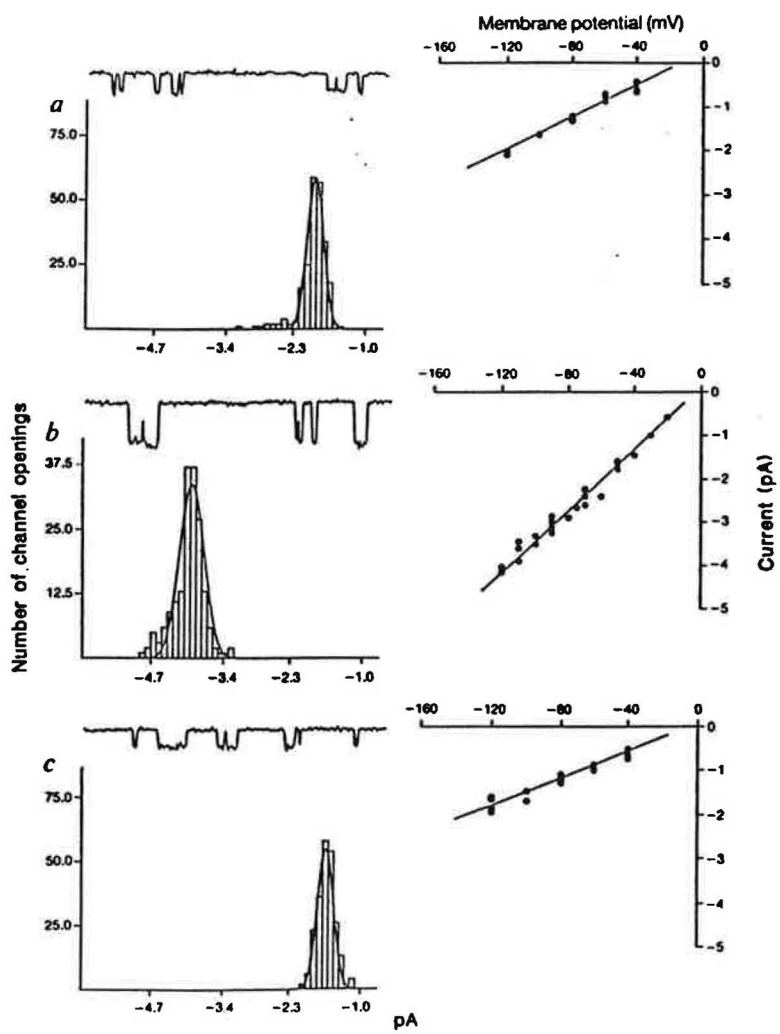

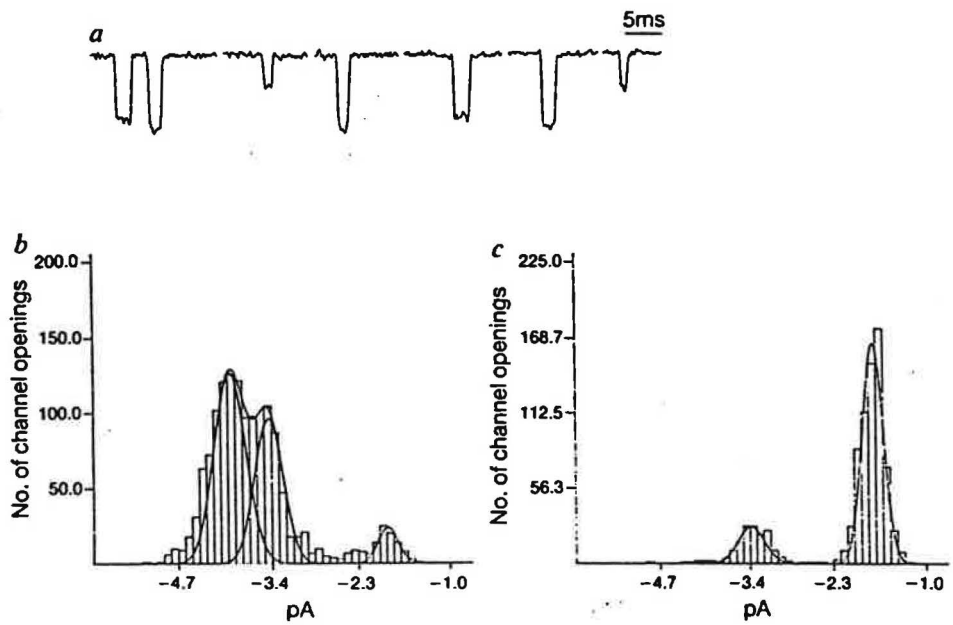

FIG. 3 Assembly of two α subunits in the functional receptor. Both α_4 and α_4K266 were coinjected with nα_1 into the same oocyte. *a*, Single channel records measured in an outside-out patch held at −120 mV and shows three receptors with different current amplitudes. *b*, Amplitude histograms of over 500 such openings. These histograms were best fitted as the sum of three gaussian distributions. The gaussian with a mean amplitude of −4.0 pA corresponds to that used to fit the α_4/nα_1E260 receptor in Fig. 2*b*. The gaussian with a mean of −1.85 pA corresponds to the gaussian used to fit the α_4K266/nα_1E260 receptor in Fig. 2*c*. The gaussian with a mean amplitude of −3.4 pA corresponds to receptors that have assembled with both α_4 and α_4K266 together with nα_1E260. The amplitude histogram in *b* was from an oocyte co-injected with equal amounts of α_4 and α_4K266. The amplitude histogram in *c* was from an oocyte co-injected with four times more α_4K266 than α_4.

incorporate α_4 subunits with nα_1E260 and others will form that incorporate $\alpha_4$266 with nα_1E260. If, however, the number of α subunits in the functional receptor is >1, then some receptors should incorporate both α_4 and α_4K266 in the same receptor. On the basis of the effect of the charge near M2 on the conductance, the single channel conductance for these receptors should be between that of the α_4/nα_1E260 receptor and that of the α_4K266/nα_1E260 receptor (see Fig. 2). If the receptor assembles with N α subunits, then there should be $N-1$ receptors expressed in the oocyte membrane which have incorporated both α_4 and α_4K266 subunits.

The results of coexpressing α_4 and α_4K266 together with nα_1E260 are shown in Fig. 3. These co-injected oocytes express receptors with three different conductances, as illustrated by the amplitude histograms in Fig. 3*b*. These histograms were best fitted as the sum of three gaussian distributions. One gaussian with a mean of −4.0 pA corresponds to that used to fit the α_4/nα_1E260 receptor (see Fig. 2*b*). One gaussian with a mean of −1.8 pA corresponds to that used to fit the α_4K266/nα_1E260 receptor (see Fig. 2*c*). The remaining gaussian has a mean intermediate between the α_4/nα_1E260 receptor and the α_4K266/nα_1E260 receptor. The simplest interpretation of this, based on the effects of charged residues at the outer edge of M2 on the single channel conductance, is that it represents a hybrid receptor that has incorporated both α_4 and α_4K266 subunits. This result was observed in all 18 patches from oocytes involving co-injection of α_4 and α_4K266 with nα_1E260, and, as shown in Fig. 3*b* and *c*, the amplitude distribution could be biased in favour of one receptor or the other by injecting differing amounts of cDNA for one subunit relative to the other. We conclude from this experiment that there are only two α subunits in the functional receptor. This is consistent with the results from the Hill coefficient measured in physiological dose-response experiments on the α_4/nα_1 receptor[7], and is identical to the two α subunit stoichiometry in muscle nAChRs[20].

The number of nα_1 subunits was assessed in a similar fashion: we coinjected nα_1 and nα_1E260 together with α_4 into oocytes

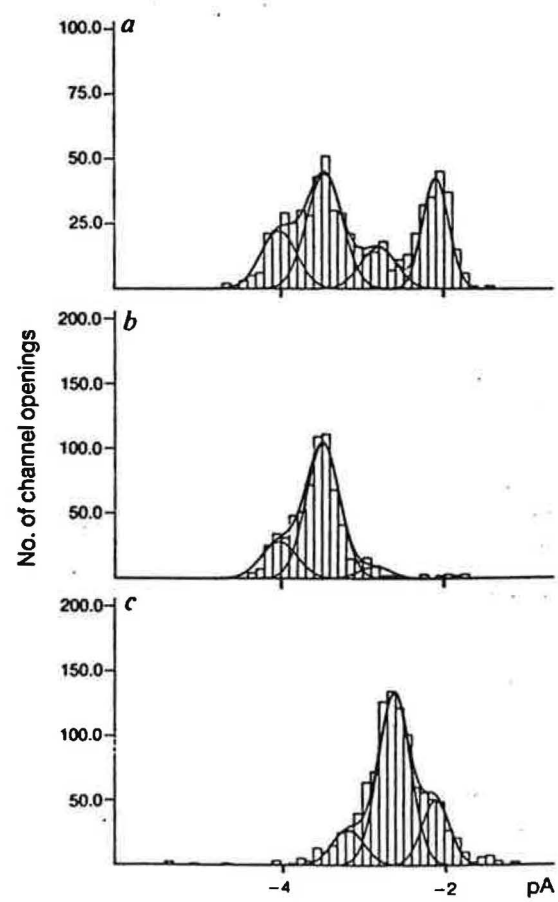

FIG. 4 The assembly of three nα_1 subunits in the functional receptor. Both nα_1 and nα_1E260 were co-injected with α_4 into the same oocyte. *a*, Results from an oocyte co-injected with equal amounts of nα_1 and nα_1E260. This histogram was best fit as the sum of four gaussian distributions. The gaussian with a mean of −4.0 pA corresponds to the α_4/nα_1E260 receptor. The gaussian with a mean of −2.0 pA corresponds to the α_4/nα_1 receptor. The gaussian with a mean of −2.7 pA corresponds to receptors that have assembled with two nα_1 subunits and one nα_1E260 subunit. The gaussian with a mean of −3.5 pA corresponds to receptors that have assembled with one nα_1 subunit and two nα_1E260 subunits. *b*, Results from an oocyte coinjected with 1.5 times more nα_1E260 than nα_1. In this histogram, the gaussian with the largest peak had a mean of −3.5 pA and corresponds to receptors that have assembled with one nα_1 subunit and two nα_1E260 subunits. *c*, Results from an oocyte coinjected with 2.5 times more nα_1 than nα_1E260. The main gaussian in this histogram had a mean of −2.7 pA and corresponds to receptors that have assembled with two nα_1 subunits and one nα_1E260 subunit.

(Fig. 4). The amplitude histograms were best fitted as the sum of four gaussians (Fig. 4*a*). The gaussian with the largest mean amplitude (−4.0 pA) corresponds to the $\alpha_4/n\alpha_1$E260 receptor (see Fig. 2*b*). The gaussian with the smallest mean amplitude (−2.0 pA) corresponds to that used to fit the wild-type $\alpha_4/n\alpha_1$ receptor (see Fig. 2*a*). The two intermediate gaussians had means of −2.7 pA and −3.5 pA. Using the same arguments based on charged residues at the outer portion of the M2 domain, the gaussian with a mean of −2.7 pA corresponds to hybrid receptors that have incorporated two $n\alpha_1$ and one $n\alpha_1$E260 subunits into the functional receptor, whereas the gaussian with a mean of −3.5 pA corresponds to receptors that have incorporated one $n\alpha_1$ and two $n\alpha_1$E260 subunits. Similar results to those in Fig. 4*a* were observed in 12 patches from oocytes co-injected with $n\alpha_1$ and $n\alpha_1$E260. In addition, the amplitude distributions could be biased in favour of one receptor subtype by injecting differing amounts of cDNA for one subunit relative to the other (Fig. 4*b* and *c*). The oocyte analysed in Fig. 4*b* predominantly expressed a receptor subtype incorporating one $n\alpha_1$ subunit and two $n\alpha_1$E260 subunits, whereas the oocyte in Fig. 4*c* mainly expressed a receptor subtype that had incorporated two $n\alpha_1$ and one $n\alpha_1$E260 subunits. Therefore, we conclude from this experiment that there are three $n\alpha$ subunits in the functional neuronal nAChRs.

The results of this study show that functional neuronal nAChRs are pentameric complexes incorporating two α subunits and three $n\alpha$ subunits. The approach taken here should also be useful in determining the stoichiometry of subunits for other ligand-gated receptors. Recently, several different α and $n\alpha$ subunits for neuronal nAChRs have been identified[6,9,10]. Our results indicate that functional neuronal nAChRs with different properties could assemble *in vivo* through the combination of different subunits. Therefore, it is conceivable that neurons may incorporate two different α subunits, coded for by different genes, or two or three different $n\alpha$ subunits into the same receptor molecule, thereby increasing the possible combinations of functionally different nAChRs expressed in the nervous system. □

Received 22 October 1990; accepted 16 January 1991.

1. Boulter, J. *et al. Nature* **319**, 368–374 (1986).
2. Noda, M. *et al. Nature* **305**, 818–823 (1983).
3. Schofield, P. R. *et al. Nature* **328**, 221–227 (1987).
4. Greenlingloh, G. *et al. Nature* **328**, 215–220 (1987).
5. Whiting, P. L. & Lindstrom, J. M. *Biochemistry* **25**, 2062–2093 (1986).
6. Wada, K. *et al. Science* **240**, 330–334 (1988).
7. Ballivet, M. *et al. Neuron* **1**, 847–852 (1988).
8. Bertrand, D., Ballivet, M. & Rungger, D. *Proc. natn. Acad. Sci. U.S.A.* **87**, 1993–1997 (1990).
9. Nef, P., Oneyser, C., Alliod, C., Couturier, S. & Ballivet, M. *EMBO J.* **7**, 595–601 (1988).
10. Boulter, J. *et al. J. biol. Chem.* **256**, 4472–4482 (1990).
11. Wada, E. *et al. J. comp. Neurol.* **284**, 314–335 (1989).
12. Whiting, P. J., Liu, R., Morely, B. J. & Lindstrom, J. M. *J. Neurosci.* **7**, 4005–4016 (1987).
13. Boulter, J. *et al. Proc. natn. Acad. Sci. U.S.A.* **84**, 7763–7767 (1987).
14. Giraudat, J., Dennis, M., Heidmann, T., Chang, S.-Y. & Changeux, J.-P. *Proc. natn. Acad. Sci. U.S.A.* **83**, 2719–2723 (1986).
15. Hucho, F. *Eur. J. Biochem.* **158**, 211–226 (1986).
16. Giraudat, J. *et al. Biochemistry* **26**, 2410–2418 (1987).
17. Leonard, R. J., Labarca, C. G., Charnet, P., Davidson, N. & Lester, H. A. *Science* **242**, 1578–1581 (1988).
18. Imoto, K. *et al. Nature* **335**, 645–548 (1988).
19. Papke, R. L., Boulter, J., Heinemann, S. & Patrick, J. *Neuron* **3**, 589–596 (1989).
20. Rafferty, M. A., Hunkapiller, M. W., Srader, C. D. & Hood, L. E. *Science* **208**, 1454–1457 (1980).
21. Zoller, M. J. & Smith, M. *DNA* **3**, 479–488 (1984).
22. Kundel, T. A. *Proc. natn. Acad. Sci. U.S.A.* **82**, 488–492 (1985).
23. Bertrand, D., Cooper, E., Valera, S., Rungger, D. & Ballivet, M. in *Electrophysiology and Microinjection: Methods in Neurosciences* (ed. Conn, P. M.) (Academic, New York, in the press).
24. Press, W. H., Flannery, B. P., Teukolsky, S. A. & Vetterling, W. T. *Numerical Recipes: The Art of Scientific Computing* (Cambridge University Press, 1986).

ACKNOWLEDGEMENTS. We thank D. Bertrand and C. R. Bader for comments on the manuscript. This work was supported by MRC of Canada, FRS du Québec and NSF of Switzerland.

Microtubule translocation in the cytokinetic apparatus of cultured tobacco cells

Tetsuhiro Asada, Seiji Sonobe & Hiroh Shibaoka

Department of Biology, Faculty of Science, Osaka University, Toyonaka, Osaka, Japan

IN higher plant cells, cytokinesis is achieved by new cross-wall formation mediated by the phragmoplast[1], a double ring of microtubules of opposite polarity, in which the short microtubules are arranged perpendicular to the equatorial plane of the phragmoplast with their plus ends interdigitating at the plane[1,2]. The phragmoplast and its enclosed cell plate move out centrifugally until the mother cell divides. We report here results of a newly developed method using glycerinated cultured tobacco cells, which show that the equatorial region of the phragmoplast can translocate microtubules towards their minus ends concomitantly with tubulin polymerization at their plus ends. The translocation is induced effectively by GTP and less effectively by ATP, and is inhibited by the unhydrolysable nucleotide analogues GMP-PNP and AMP-PNP. Thus, the equatorial region of the phragmoplast seems to be associated with a mechanochemical enzyme that generates the force for microtubule translocation by hydrolysing GTP.

Cultured tobacco cells with phragmoplasts were treated with glycerin to permeabilize the plasma membrane[3] and DTAF (dichlorotriazonilamino fluoroscein)-labelled tubulin was introduced into the glycerinated cells. Although cytokinetic progression was arrested by glycerination, an array of phragmoplast microtubules was well preserved in the glycerinated cells, as judged by anti-tubulin immunofluorescence (Fig. 1*f*). As has been reported[1], there was no staining of the equatorial region where microtubules are interdigitating with their plus ends (Fig. 1*f*).

A bright fluorescent band appeared at the equatorial region of the phragmoplast in the glycerinated cells incubated with DTAF-tubulin (Fig. 1*a*), suggesting that DTAF-tubulin polymerizes onto the plus ends of pre-existing phragmoplast microtubules. Weak, broad fluorescence appeared at the distal portions of the phragmoplasts (Fig. 1*b*, *c*), suggesting that polymerization also occurs at the minus ends (Fig. 4*a*). The width of the bright band at the equatorial plane increased with time (Fig. 1*a*–*c*), and the distal, broad fluorescent bands moved away from the equatorial plane (Fig. 1*b*, *c*), suggesting that the microtubules are translocated towards their minus ends concomitantly with tubulin polymerization onto their plus ends. Microtubule translocation was more clearly shown by the experiment in which cells like the one in Fig. 1*b* were further incubated with unlabelled tubulin. The fluorescent band at the equatorial region is split in two by a newly formed, unlabelled band and each of the resultant pair of fluorescent bands is translocated away from the equatorial plane (Figs 1*d*, *e*; and 4*b*). Figure 2*a* shows that the unlabelled band appears after a short lag period, during which the interdigitating portions of fluorescent microtubules move apart, and increases its width with time. The rate of translocation seems to depend on the rate of polymerization when the tubulin concentration is lower than 0.5 mg ml^{-1}. The separation of the fluorescent band does not occur in the absence of unlabelled tubulin (Fig. 2*a*). But when the tubulin concentration is 0.5 mg ml^{-1} or higher, the rate of translocation seems to be limited by the activity of the microtubule-translocating system.

In the presence of GMP-PNP or AMP-PNP, phragmoplasts